

Article

Complexity of switching chaotic maps in finite precision

M. Antonelli ^{1,2,*} , L. De Micco ^{1,2,3}, H. A. Larondo ^{1,2,3} and O. A. Rosso ^{3,4,5,6}

¹ Facultad de Ingeniería, Universidad Nacional de Mar del Plata (UNMdP), Mar del Plata, Argentina.

² ICyTE. Instituto de Investigaciones Científicas y Tecnológicas en Electrónica.

³ CONICET. Consejo Nacional de Investigaciones Científicas y Técnicas.

⁴ Departamento de Informática en Salud, Hospital Italiano de Buenos Aires, Ciudad Autónoma de Buenos Aires, Argentina.

⁵ Instituto de Física, Universidade Federal de Alagoas (UFAL), Maceió, Brazil.

⁶ Facultad de Ingeniería y Ciencias Aplicadas, Universidad de Los Andes, Santiago, Chile.

* Correspondence: maxanto@fimdp.edu.ar

Academic Editor: name

Version December 26, 2017 submitted to Entropy

Abstract: In this paper we investigate the degradation of the statistic properties of chaotic maps as consequence of their implementation in a digital media such as Digital Signal Processors (DSP), Field Programmable Gate Arrays (FPGA) or Application-Specific Integrated Circuits (ASIC). In these systems, binary floating- and fixed-point are the numerical representations available. Fixed-point representation is preferred over floating-point when speed, low power and/or small circuit area are necessary. Then, in this paper we compare the degradation of fixed-point binary precision version of chaotic maps with the floating point IEEE754 to evaluate the feasibility of their FPGA implementation. The specific period that every fixed-point precision produces was investigated in previous reports, using as example the tent map and the logistic map. Statistical characteristics are also relevant. It has been recently shown that it is convenient to describe the statistical characteristic using both, causal and non-causal quantifiers. In this paper we complement the period analysis by characterizing the behavior of these maps from a statistical point of view using causal and non-causal entropies and complexities. Here we do not look for the system to be similar to the implemented in real numbers, but that certain conditions related to the statistics of systems are met.

Keywords: chaos; finite precision; hardware implementaion; switching maps

1. Introduction

In the last years digital systems became the standard in all experimental sciences. By using new programmable electronic devices such as Digital Signal Processors (DSP), Application Specific Integrated Circuits (ASIC) or Field Programmable Gate Array FPGA's, experimenters are allowed to design and modify their own signal generators, measuring systems, simulation models, etc.

Nowdays, the chaotic systems are widely used in digital electronics in fields such as electromagnetic compatibility, encrypted secure communications, controlled noise generators, etc [1–6]. These systems are specially interesting due to their extreme sensibility to initial conditions, nevertheless this characteristic is the source of the main difficulties at the time to implement them. In these fields of the electronic, the focus is not on how similar is the system implemented with a system in real numbers, but on some properties of the implemented system meet certain requirements.

When a chaotic system is implemented in computers or any digital device, the chaotic attractor become periodic by the effect of finite precision, then only pseudo chaotic attractors can be generated

[7,8]. Discretization may even destroy the pseudo chaotic behavior and consequently is a non trivial process [3,9].

In these new devices, floating- and fixed-point are the available arithmetic. Floating-point is the more accurately solution but is not always recommended when speed, low power and/or small circuit area are required. A fixed-point solution is better in these cases, nevertheless the feasibility of their implementation needs to be investigated.

The effect of numerical discretization over a chaotic map was recently addressed in [7], [3] and [10]. In our previous work [3] we have explored the statistical degradation of the phases' space for a family of 2D quadratic maps. These maps present a multiattractor dynamic that makes them very attractive as random number generator in fields like criptography, encoding, etc. Nepomuceno *et al.* [10] reported the existence of more than one pseudo-orbit of continuous chaotic systems when it is discretized using different schemes.

Grebogi and coworkers [12] saw that the period T scales with roundoff ϵ as $T \sim \epsilon^{-d/2}$ where d is the correlation dimension of the chaotic attractor. This issue was also addressed in [13], in this paper authors explore the evolution on the period T as consequence of roundoff induced by 2-based numerical representation. To have a large period T is an important property of chaotic maps, in [14] Nagaraj *et. al* studied the effect of switching over the average period lengths of chaotic maps in finite precision. They saw that the period T of the compound map obtained by switching between two chaotic maps is higher than the period of each map. Liu *et. al* [15] studied different switching rules applied to linear systems to generate chaos. Switching issue was also addressed in [16], the author considered some mathematical, physical and engineering aspects related to singular, mainly switching systems. Switching systems naturally arise in power electronics and many other areas in digital electronics. They have also interest in transport problems in deterministic ratchets [17] and it is known that synchronization of the switching procedure affects the output of the controlled system. Chiou and Chen [18] published an analysis of the stabilization and switching laws to design switched discrete-time systems. Recently, Borah *et al.* [19] presented a family of new chaotic systems and a switching based synchronization strategy.

Stochasticity and mixing are relevant to characterize a chaotic behavior. To investigate these properties several quantifiers were studied [20]. Entropy and complexity from information theory were applied to give a measure for causal and non causal entropy and causal complexity.

A fundamental issue is the criterium to select the probability distribution function (PDF) assigned to the time series, causal and non causal options are possible. Here we consider the non causal traditional PDF obtained by normalizing the histogram of the time series. Its statistical quantifier is the normalized entropy H_{hist} that is a measure of equiprobability among all allowed values. We also considered a causal PDF that is obtained by assigning ordering patterns to segments of trajectory of length D . This PDF was first proposed by Bandt & Pompe in a seminal paper [21]. The corresponding entropy H_{BP} was also proposed as a quantifier by Bandt & Pompe, in [22] authors applied the causal complexity C_{BP} to detect chaos. Among them the use of an entropy-complexity representation ($H_{hist} \times C_{BP}$ plane) and causal-non causal entropy ($H_{BP} \times H_{hist}$ plane) deserves special consideration [20,22–27].

Recently, amplitude information was introduced in [28] to add some immunity to weak noise in a causal PDF. The new scheme better tracks abrupt changes in the signal and assigns less complexity to segments that exhibit regularity or are subject to noise effects. Then, we define the causal entropy with amplitude contributions H_{BPW} and the causal complexity with amplitude contributions C_{BPW} . Also, we introduce the modified planes $H_{hist} \times C_{BP}$ and $H_{BP} \times H_{hist}$.

Amigó and coworkers proposed the number of forbidden patterns as a quantifier of chaos [29]. Essentially they reported the presence of forbidden patterns as an indicator of chaos. Recently it was shown that the name forbidden patterns is not convenient and it was replaced by missing patterns (MP) [30], in this work authors showed that there are chaotic systems that present MP from a certain

78 minimum length of patterns. Our main interest on MP is because it gives an upper bound for causal
79 quantifiers.

80 Following [14], in this paper we study the statistical characteristics of five maps, two well known
81 maps: (1) the tent (TENT) and (2) logistic (LOG) maps, and three additional maps generated from
82 them: (3) SWITCH, generated by switching between TENT and LOG; (4) EVEN, generated by skipping
83 all the elements in odd positions of SWITCH time series and (5) ODD, generated by discarding all the
84 elements in even positions of SWITCH time series. Binary floating- and fixed-point numbers are used,
85 these specific numerical systems may be implemented in modern programmable logic devices.

86 The main contribution of this paper is the study of how different statistical quantifiers detect the
87 evolution of stochasticity and mixing of the chaotic maps according as the numerical precision varies.
88 To illustrate this sequences generated by well known maps were used, and also sequences obtained by
89 randomization methods like skipping and switching.

90 Organization of the paper is as follows: Section 2 describes the statistical quantifiers used in
91 the paper and the relationship between their value and the characteristics of the causal and non
92 causal PDF's considered; Section 3 shows and discusses the results obtained for all the numerical
93 representations. Finally Section 4 deals with final remarks and future work.

94 2. Information theory quantifiers

95 Systems that evolve over time are called dynamical systems. Generally, only measurements of
96 scalar time series $X(t)$ are accessible, these time series may be function of variables $V = \{v_1, v_2, \dots, v_k\}$
97 describing the underlying dynamics (i.e. $dV/dt = f(V)$). The goal is to infer properties and reach
98 conclusions of an unknown system from the analysis of measured record of observational data. The key
99 question would be to know how much information about the dynamics of the underlying processes
100 can be revealed by the analysed data. A probability distribution function (PDF) P is typically used to
101 quantify the apportionment of a time series $X(t)$. Information Theory quantifiers can be defined as
102 measures that characterize properties of the PDF associated with these time series, they allow to extract
103 information about the studied system. We can see these quantifiers as metrics in the PDFs space, they
104 enable to compare and classify different sets of data according to their PDFs where stochastic and
105 deterministic are the two extremes of processes.

106 Here, we are concerned in chaotic dynamics, which are fundamentally *causal* and *statistical* in
107 nature. For this reason, we are forced to use a different approach since a purely statistical approach
108 ignores the correlations between successive values from the time series; and a causal approach focuses
109 on the PDFs of data sequences.

110 The selected quantifiers are based on symbolic counting and ordinal pattern statistics. They make
111 it possible to distinguish between the two main features: the *information content* of data and their
112 *complexity*. It is important to highlight that rather than referring to a physical space, here we talk about
113 a space of probability density functions.

114 In this section, we will introduce Information Theory quantifiers defined over discrete PDFs since
115 discrete time series is our scope. Nevertheless, in [31] definitions for the continuous case can be found.

116 2.1. Shannon entropy and statistical complexity

117 Entropy is a measure of the uncertainty associated with a physical process that is described by
118 P . The Shannon entropy is considered as the most natural one [31] when dealing with information
119 content.

Let define a discrete probability distribution $P = \{p_i; i = 1, \dots, N\}$ with $\sum_{i=1}^N p_i = 1$, were N is
the number of possible states of the system under study. Then, Shannon's logarithmic information
measure:

$$S[P] = - \sum_{i=1}^N p_i \ln [p_i] \quad (1)$$

When $S[P] = S_{\min} = 0$, the prediction of which outcome i will occur is a complete certainty. In this case, it is maximal the knowledge of the underlying process described by the probability distribution. On the contrary, we have minimal knowledge in a case of a uniform distribution $P_e = \{p_i = 1/N; i = 1, \dots, N\}$ since every outcome has the same probability of occurrence, and the uncertainty is maximal, i.e., $S[P_e] = S_{\max} = \ln N$. These two situations are extreme cases, therefore we focus on the ‘normalized’ Shannon entropy, $0 \leq H \leq 1$, given as

$$H[P] = S[P]/S_{\max} \quad (2)$$

On the other hand, there is not a unique definition of the concept of complexity. In this paper, the aim is to describe the complexity of the time series rather than that of the underlying systems. As stated by Kantz [32], complex data might be generated by “simple” systems, while “complicated” models can generate low complexity outputs. A quantitative complexity can be defined as a measure that assigns low values both to uncorrelated random data (maximal Shannon entropy) and also to perfectly ordered data (null Shannon entropy). Then, if we have an ordered sequence, such as a simple oscillation or trend, the statistical complexity would be low, and the same would happen with an unordered sequence, such as uncorrelated white noise. In the middle of this situation the characterization of data is more difficult hence the complexity would be higher.

We look forward a quantifier functional of a PDF, $C[P]$, in order to measure the degree of complexity or of correlational structures. As depicted in [33] the functional is relate to organization, correlational structure, memory, regularity, symmetry, patterns, and other properties.

Rosso and coworkers [34] introduced a suitable *Statistical Complexity Measure* (SCM) C , that is based on the seminal notion advanced by López-Ruiz *et al.* [35]. SCM is defined as the product of a measure of information and a measure of disequilibrium and it is able to detect the distance from the equiprobable distribution of the accessible states.

This statistical complexity measure [34,36] is defined as follows:

$$C[P] = Q_J[P, P_e] \cdot H[P] \quad (3)$$

H is the normalized Shannon entropy, see eq. 2, and Q_J is the disequilibrium defined in terms of the Jensen-Shannon divergence $J[P, P_e]$, [37]. That is,

$$Q_J[P, P_e] = Q_0 J[P, P_e] = Q_0 \{S[(P + P_e)/2] - S[P]/2 - S[P_e]/2\} \quad (4)$$

Q_0 is a normalization constant such that $0 \leq Q_J \leq 1$:

$$Q_0 = -2 \left\{ \frac{N+1}{N} \ln(N+1) - \ln(2N) + \ln N \right\}^{-1} \quad (5)$$

This value is obtained in a totally deterministic situation, where only one components of P has a no null value equal to one.

Note that the above introduced SCM depends on two different probability distributions: one associated with the system under analysis, P , and the other with the uniform distribution, P_e . Furthermore, it was shown that for a given value of H , the range of possible C values varies between a minimum C_{\min} and a maximum C_{\max} , restricting the possible values of the SCM [38]. Thus, it is clear that important additional information related to the correlational structure between the components of the physical system is provided by evaluating the statistical complexity measure.

2.2. Determination of a probability distribution

The evaluation derived from the Information Theory quantifiers suppose some prior knowledge about the system; specifically for those previously introduced (Shannon entropy and statistical

complexity), a probability distribution associated to the time series under analysis should be provided before.

The determination of the most adequate PDF is a fundamental problem because the PDF P and the sample space Ω are inextricably linked.

Usual methodologies assign to each value of the series $X(t)$ (or non-overlapped set of consecutive values) a symbol from a finite alphabet $A = \{a_1, \dots, a_M\}$, thus creating a *symbolic sequence* that can be regarded to as a *non causal coarse grained* description of the time series under consideration. In this case, information on the dynamics of the system is lost, such as order relations and the time scales.

If we want to incorporate *Causal information* we have to add information about the past dynamics of the system, this is done by the assignment of symbols of alphabet A to a portion of the trajectory. The Bandt and Pompe (BP) [21] method is a simple and robust methodology that compares neighboring values in a time series and, thus solves this issue.

The causality property of the PDF allows quantifiers (based on this PDFs) to discriminate between deterministic and stochastic systems [39]. The steps are, first it is needed to create symbolic data by ranking the values of the series; and second to define by reordering the embedded data in ascending order. This last step is the same to make a phase space reconstruction, using embedding dimension D (pattern length) and time lag τ . The goal of quantifying the diversity of the ordering symbols is achieved. There is no need to perform model-based assumptions, because the appropriate symbol sequence arises naturally from the time series.

The procedure is the following:

- Given a series $\{x_t; t = 0, \Delta t, \dots, N\Delta t\}$, a sequence of vectors of length D is generated.

$$(s) \longmapsto (x_{t-(d-1)\Delta t}, x_{t-(d-2)\Delta t}, \dots, x_{t-\Delta t}, x_t) \quad (6)$$

Each vector turns out to be the “history” of the value x_t . Clearly, the longer the length of the vectors D , the more information about the history would the vectors have but a higher value of N is required to have an adequate statistics.

- The permutations $\pi = (r_0, r_1, \dots, r_{D-1})$ of $(0, 1, \dots, D-1)$ are called “order of patterns” of time t , defined by:

$$x_{t-r_{D-1}\Delta t} \leq x_{t-r_{D-2}\Delta t} \leq \dots \leq x_{t-r_1\Delta t} \leq x_{t-r_0\Delta t} \quad (7)$$

In order to obtain an unique result it is considered $r_i < r_{i-1}$ if $x_{t-r_i\Delta t} = x_{t-r_{i-1}\Delta t}$. In this way, all the $D!$ possible permutations π of order D , and the PDF $P = \{p(\pi)\}$ is defined as:

$$p(\pi) = \frac{\#\{s | s \leq N - D + 1; (s) \text{ has type } \pi\}}{N - D + 1} \quad (8)$$

In the last expression the $\#$ symbol denotes cardinality.

From the time series an ordinal pattern probability distribution $P = \{p(\pi_i), i = 1, \dots, D!\}$ is extracted. For this, a unique symbol π is obtained from the vector defined by eq. 8. For uniqueness, $r_i < r_{i-1}$ if $x_{s-r_i} = x_{s-r_{i-1}}$ is defined. With the following stationary assumption: for $k \leq D$, the probability for $x_t < x_{t+k}$ should not depend on t need to be met for the applicability of the BP method. Regarding the selection of the parameters, Bandt and Pompe suggested working with $3 \leq D \leq 6$ for typical time series lengths, and specifically considered a time lag $\tau = 1$ in their cornerstone paper.

Recently, the permutation entropy was extended to incorporate amplitude information. In order to avoid the loss of amplitude information, that would be a disadvantage of ordinal pattern statistics, weights are introduced to obtain a “weighted permutation entropy (WPE)” [28].

Non-normalized weights are computed for each temporal window for the time series X , such that

$$w_j = \frac{1}{D} \sum_{k=1}^D (x_{j+k-1} - \bar{X}_j^D)^2 \quad (9)$$

180 In the equation above $x_{j+k-1} - \bar{X}_j^D$ denotes the arithmetic mean of the current embedding vector of
 181 length D and its variance w_j is then used to weight the relative frequencies of each ordinal pattern
 182 p_j . Originally, this technique was proposed to discriminate patterns immersed in low noise. We take
 183 advantage of the fact that the fixed points are not computed in the WPE.

184 We calculated the normalized permutation Shannon entropy H and the statistical complexity C
 185 from these PDFs, and the obtained values are denoted as:

- 186 • H_{hist} , is the normalized Shannon entropy applied to non-causal PDF P_{hist}
- 187 • H_{BP} , is the normalized Shannon entropy applied to causal PDF P_{BP}
- 188 • H_{BPW} , is the normalized Shannon entropy applied to causal PDF with amplitude contribution
 P_{BPW}
- 189 • C_{BP} , is the normalized statistical complexity applied to causal PDF P_{BP}
- 190 • C_{BPW} , is the normalized statistical complexity applied to causal PDF with amplitude contribution
 P_{BPW}

193 2.3. Information Planes

194 A particularly useful visualization of the quantifiers from Information Theory is their juxtaposition
 195 in two-dimensional graphs. Four information planes are defined:

- 196 1. Causal entropy vs. non-causal entropy, $H_{BP} \times H_{hist}$
- 197 2. Causal entropy with amplitude contributions vs. non-causal entropy, $H_{BPW} \times H_{hist}$
- 198 3. Causal causal complexity vs. causal entropy, $C_{BP} \times H_{BP}$
- 199 4. Causal causal complexity with amplitude contributions vs. causal entropy with amplitude
 P_{BPW}

200 These diagnostic tools were shown to be particularly efficient to distinguish between the
 201 deterministic chaotic and stochastic nature of a time series since the permutation quantifiers have
 202 distinct behaviors for different types of processes.

203 In Figure 1 we show the planes $H_{BP} \times H_{hist}$ and $H_{BPW} \times H_{hist}$ overlapped. In the resulting plane
 204 a higher value in any of the entropies, H_{BP} , H_{BPW} or H_{hist} , implies a more uniformity in the involved
 205 PDF. The point $(1, 1)$ represents the ideal case with uniform histogram and uniform distribution of
 206 ordering patterns. We show some relevant points as example. Ideal white random sequences with
 207 uniform distribution gives a point at $(H_{hist}, H_{BP}) = (1, 1)$ represented by a blue circle, a red circle in
 208 the same position shows the results when amplitude contributions are included $(H_{hist}, H_{BPW}) = (1, 1)$.
 209 If we sort the vector generated by ideal white random generator in an ascendant way, resulting points
 210 are shown by a blue square $(H_{hist}, H_{BP}) = (1, 0)$ and a red square $(H_{hist}, H_{BPW}) = (1, 0)$, in both
 211 cases the squares are overlapped at point $(1, 0)$ this example illustrates the complementarity of the
 212 information provided by H_{hist} and H_{BP} .

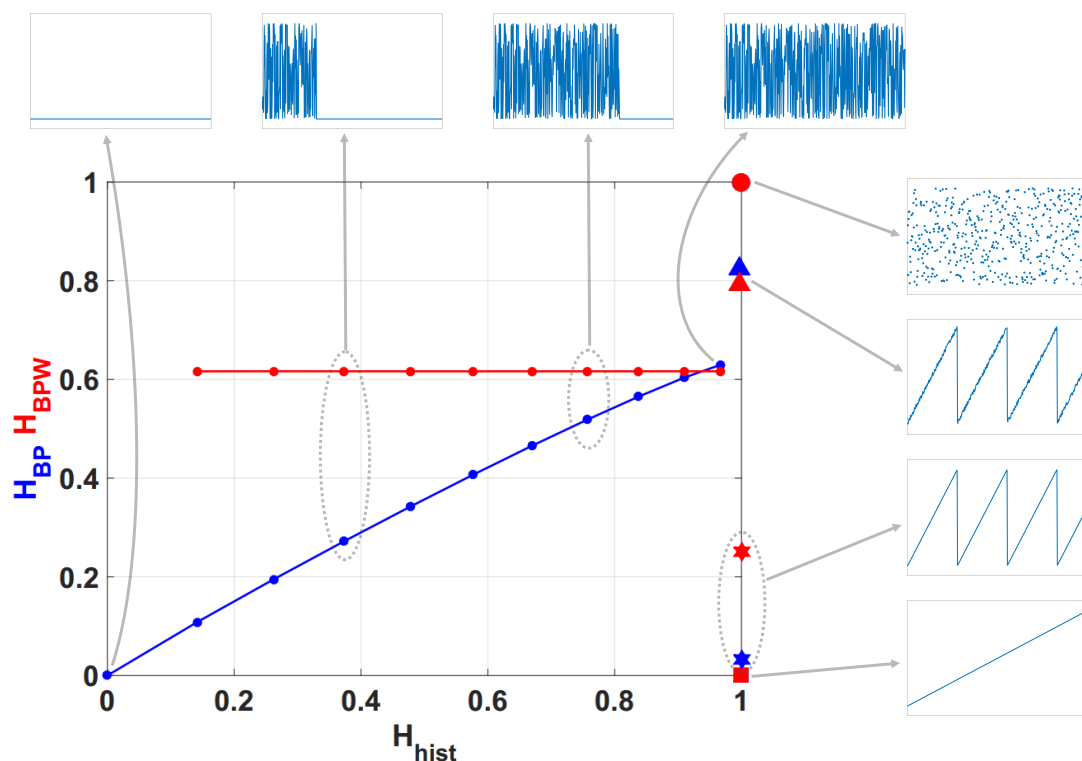


Figure 1. Causal-Non causal Entropy plane, values of the quantifiers for some characteristic signals, from purely deterministic through purely random (see text).

214 Blue and red stars show (H_{hist}, H_{BP}) and (H_{hist}, H_{BPW}) respectively, applied to a sawtooth signal.
 215 Values are perfectly distributed in all interval but only a few ordering patterns appear, this explains the
 216 high H_{hist} and low H_{BP} . The frequency of occurrence of low amplitude patterns is higher than the one
 217 of high amplitude patterns, then the PDF with amplitude contributions is more uniform and H_{BPW} is
 218 a little higher than H_{BP} . When sawtooth signal is contaminated with white noise H_{BP} and H_{BPW} are
 219 increased as shown with blue and red triangles. Clearly, new ordering patterns appear and both H_{BP}
 220 and H_{BPW} show higher values than non-contaminated case. However the growth of H_{BPW} is smaller
 221 than H_{BP} showing that the technique of recording amplitude contributions adds some immunity to
 222 noise.

223 Finally, we evaluated the quantifiers for a sequence of a logistic map that converges to a fixed point,
 224 in all cases the length of data vector remains constant and the length of transitory is variable. Results
 225 obtained without amplitude contributions are depicted in blue dots, they converge to $(H_{hist}, H_{BP}) =$
 226 $(0, 0)$ as the length of transitory is shorter, however H_{BPW} (in red points) remains constant for all the
 227 cases. The last point in $(H_{hist}, H_{BP}) = (0, 0)$ corresponds to a vector of zeros, in this case the histogram
 228 of ordering patterns with amplitude contributions is also a zero vector and H_{BPW} can not be calculated.
 229 Through this last example, we show that the convergence to a fixed point can be detected by the joint
 230 information of H_{BP} and H_{BPW} .

231 In Figure 2 we show the causality plane $H_{BP} \times C_{BP}$. We can see that not the entire region
 232 $0 < H_{BP} < 1, 0 < C_{BP} < 1$ is achievable, in fact, for any PDF the pairs (H, C) of possible values fall
 233 between two extreme curves in the plane $H_{BP} \times C_{BP}$ [40].

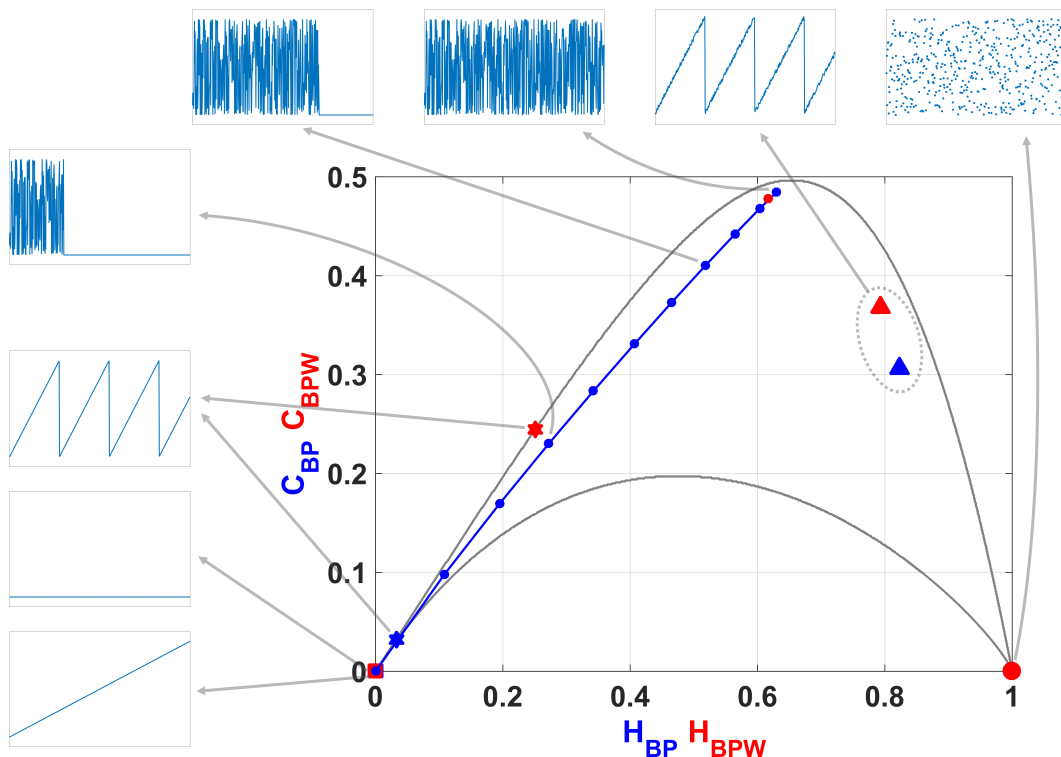


Figure 2. Causal Entropy-Complexity plane, values of the quantifiers for some characteristic signals, from purely deterministic through purely random (see text).

Chaotic maps present high values of complexity C_{BP} (close to the upper complexity limit), and intermediate entropy H_{BP} [22,41]. In the case of regular processes the values of entropy and complexity are close to zero. Stochastic processes that are uncorrelated present H_{BP} near one and C_{BP} near zero.

Ideal random systems having uniform Bandt & Pompe PDF, are represented by the point $(1,0)$ [42] and a delta-like PDF corresponds to the point $(0,0)$. In Figure 2 we show $H_{BP} \times C_{BP}$ with and without amplitude contributions. The same sample points are showed to illustrate the planar positions for different data vectors.

In both information planes $H_{BP} \times H_{hist}$ in Figure 1 and $H_{BP} \times C_{BP}$ in Figure 2, stochastic, chaotic and deterministic data are clearly localized at different planar positions.

We also used the number of missing patterns MP as a quantifier [30]. As shown recently by Amigó *et al.* [43–46], in the case of deterministic maps, not all the possible ordinal patterns can be effectively materialized into orbits, which in a sense makes these patterns missing. Indeed, the existence of these missing ordinal patterns becomes a persistent fact that can be regarded as a new dynamical property. Thus, for a fixed pattern-length (embedding dimension D) the number of missing patterns of a time series (unobserved patterns) is independent of the series length N . Remark that this independence does not characterize other properties of the series such as proximity and correlation, which die out with time [44,46]. A complete description and discussion about these quantifiers can be found in [23,26,30,35,38,47–49].

3. Results

Five pseudo chaotic maps were studied, two simple maps and three combination of them. For each one we have used numbers represented by floating-point (double precision 754-IEEE standard) and fixed-point numbers with $1 \leq B \leq 53$, where B is the number of bits that represents the fractional

²⁵⁶ part. Time series were generated using 100 randomly chosen initial conditions within their attraction
²⁵⁷ domain (interval $[0, 1]$), for each one of these 54 number precisions.

²⁵⁸ The studied maps are logistic (LOG), tent (TENT), sequential switching between TENT and LOG
²⁵⁹ (SWITCH) and skipping discarding the values in the odd positions (EVEN) or the values in the even
²⁶⁰ positions (ODD) respectively.

Logistic map is interesting because it is representative of the very large family of quadratic maps.
 Its expression is:

$$x_{n+1} = 4x_n(1 - x_n) \quad (10)$$

²⁶¹ with $x_n \in \mathbb{R}$.

Note that to effectively work in a given representation it is necessary to change the expression of the map in order to make all the operations in the chosen representation numbers. For example, in the case of LOG the expression in binary fixed-point numbers is:

$$x_{n+1} = 4\epsilon \text{ floor} \left\{ \frac{x_n(1 - x_n)}{\epsilon} \right\} \quad (11)$$

²⁶² with $\epsilon = 2^{-B}$ where B is the number of bits that represents the fractional part.

²⁶³ Floating point representation does not constitute a field, wherein the basic maths properties, such
²⁶⁴ as distributive, associative, are preserved. However, in fixed point arithmetics the exponent does not
²⁶⁵ shift the point position and some properties as distributive remains. Also, we adopt the floor rounding
²⁶⁶ mode because it arises naturally in a FPGA implementation.

²⁶⁷ The TENT map has been extensively studied in the literature because theoretically it has nice
²⁶⁸ statistical properties that can be analytically obtained. For example it is easy to proof that it has
²⁶⁹ a uniform histogram and consequently an ideal $H_{hist} = 1$. The Perron-Frobenius operator and its
²⁷⁰ corresponding eigenvalues and eigenfunctions may be analytically obtained for this map [50].

Tent map is represented with the equation:

$$x_{n+1} = \begin{cases} 2x_n & , \text{if } 0 \leq x_n \leq 1/2 \\ 2(1 - x_n) & , \text{if } 1/2 < x_n \leq 1 \end{cases} \quad (12)$$

²⁷¹ with $x_n \in \mathbb{R}$.

In base-2 fractional numbers rounding, equation (12) becomes:

$$x_{n+1} = \begin{cases} 2x_n & , \text{if } 0 \leq x_n \leq 1/2 \\ \epsilon \text{ floor}\left\{ \frac{2 - 2x_n}{\epsilon} \right\} & , \text{if } 1/2 < x_n \leq 1 \end{cases} \quad (13)$$

²⁷² with $\epsilon = 2^{-B}$.

²⁷³ In this case, we introduce the 2 number in the parentheses because it is computationally more
²⁷⁴ efficient in a hardware implementation. It is valid because it is power of 2 and the multiplication is
²⁷⁵ equivalent to a shift-to-left.

²⁷⁶ Switching, even and odd skipping procedures are shown in Fig. 3.

SWITCH map is expressed as:

$$\begin{cases} x_{n+1} = \begin{cases} 2x_n, & , \text{if } 0 \leq x_n \leq 1/2 \\ 2(1 - x_n) & , \text{if } 1/2 < x_n \leq 1 \end{cases} \\ x_{n+2} = 4x_{n+1}(1 - x_{n+1}) \end{cases} \quad (14)$$

²⁷⁷ with $x_n \in \mathbb{R}$ and n an even number.

²⁷⁸ Skipping is a usual randomizing technique that increases the mixing quality of a single map
²⁷⁹ and correspondingly increases the value of H_{BP} and decreases C_{BP} of the time series. Skipping does

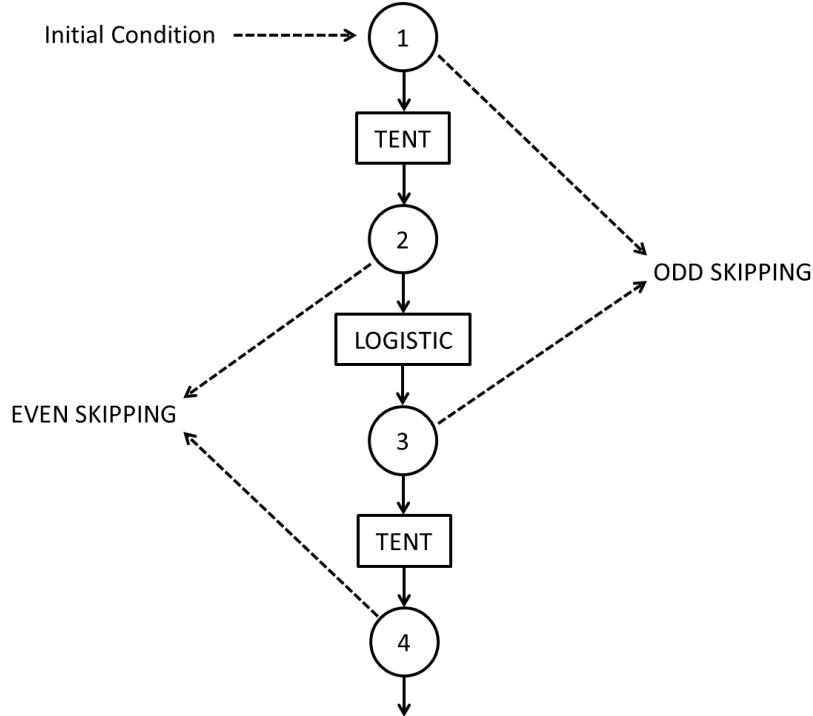


Figure 3. Sequential switching between Tent and Logistic maps. In the figure are also shown even and odd skipping strategies.

not change the values of H_{hist} for ergodic maps because it are evaluated using the non causal PDF (normalized histogram of values) [23].

In the case under consideration we study even and odd skipping of the sequential switching of TENT and LOG maps:

1. Even skipping of the sequential switching of Tent and Logistic maps (EVEN). If $\{x_n; n = 1, \dots, \infty\}$ is the time series generated by eq. (14), discard all the values in odd positions and retain the values in even positions.
2. Odd skipping of the sequential switching of Tent and Logistic maps. If $\{x_n; n = 1, \dots, \infty\}$ is the time series generated by eq. (14), discard all the values in even positions and retain all the values in odd positions.

Even skipping may be expressed as the composition function $TENT \circ LOG$ while odd skipping may be expressed as $LOG \circ TENT$. The evolution of period as function of precision was reported in [14].

Let us detail our results for each of these maps.

3.1. Period as a function of binary precision

Grebogi and coworkers [12] have studied how the period T is related with the precision. There they saw that the period T scales with roundoff ϵ as $T \sim \epsilon^{-d/2}$ where d is the correlation dimension of the chaotic attractor.

Nagaraj *et al.* [14] studied the case of switching between two maps. They saw that the period T of the compound map obtained by switching between two chaotic maps is higher than the period of each map and they found that a random switching improves the results. Here we have considered sequential switching to avoid the use of another random variable, because it can include its own statistical properties in the time series.

Figure 4 shows T vs. B in semi logarithmic scale. We run the attractor of the LOG from 100 randomly chosen initial conditions. The figure show: 100 red points for each fixed-point precision

($1 \geq B \geq 53$) and their average (dashed black line connecting black dots). The experimental averaged points can be fitted by a straight line (in blue) expressed as $\log_{10} T = mB + b$ where m is the slope and b is the y -intercept. Results for all the considered maps are summarized in Table 1.

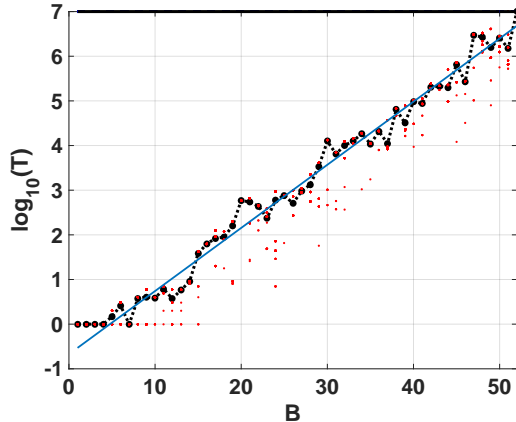


Figure 4. Period as function of precision in binary digits (see text).

Table 1. Period T as a function of B for the maps considered

map	m	b
TENT	0	0
LOG	0.139	-0.6188
SWITCH	0.1462	-0.5115
EVEN	0.1447	-0.7783
ODD	0.1444	-0.7683

Results are compatible for those obtained in [14]. Switching between maps increases the period T but skipping procedure decreases by almost half.

3.2. Quantifiers of simple maps

Here we report our results for both simple maps, LOG and TENT

3.2.1. LOG

Figures 5a to 5f show the statistical properties of LOG map in floating-point and fixed-point representation. All these figures show: 100 red points for each fixed-point precision ($1 \geq B \geq 53$) and in black their average (dashed black line connecting black dots), 100 horizontal dashed blue lines that are the results of each run in floating-point and a black solid line their average. Note that these lines are independent of x-axis. In this case, all the lines of the floating-point are overlapped.

According as B grows, statistical properties vary until they stabilize. For $B \geq 30$ the value of H_{hist} remains almost identical to the value for the floating-point representation whereas H_{BP} and C_{BP} stabilizes at $B > 21$. Their values are: $\langle H_{hist} \rangle = 0.9669$; $\langle H_{BP} \rangle = 0.6269$; $\langle C_{BP} \rangle = 0.4843$. Note that the stable value of missing patterns $MP = 645$ makes the optimum $H_{BP} \leq \ln(75) / \ln(720) \simeq 0.65$. Then, $B = 30$ is the most convenient choice for hardware implementation because an increase in the number of fractional digits does not improve the statistical properties.

Some conclusions can be drawn regarding BP and BPW quantifiers. For $B = 1, 2, 3$ and 4, the averaged BP quantifiers are almost 0 while the averaged BPW quantifiers can not be calculated (see in Figures 5c and 5e the missing black dashed line). This is because for those sequences were the initial

326 condition were 0 all iterations result to be a sequence of zeros (the fixed point of the map), this is more
327 likely to happen when using small precisions because of roundoff.

328 When B increases the initial conditions are rounded to zero less frequently, this can be seen for
329 $B > 6$. In this, case the generated sequences starting from a non-null value fall to zero after a short
330 transitory very often. An interesting issue in Figures 5c and 5e, is that BPW quantifiers show a high
331 dispersion unlike BP quantifiers. This is because BPW procedure takes into account the transient and
332 discards fixed points, unlike BP procedure considers all the values of the sequence. We can see in
333 Figures 5c and 5e for $1 < B < 10$ horizontal lines of red points that do not appear in Figures 5b and 5d,
334 this evidences that different initial conditions fall to the same orbits, even for adjacent precisions.

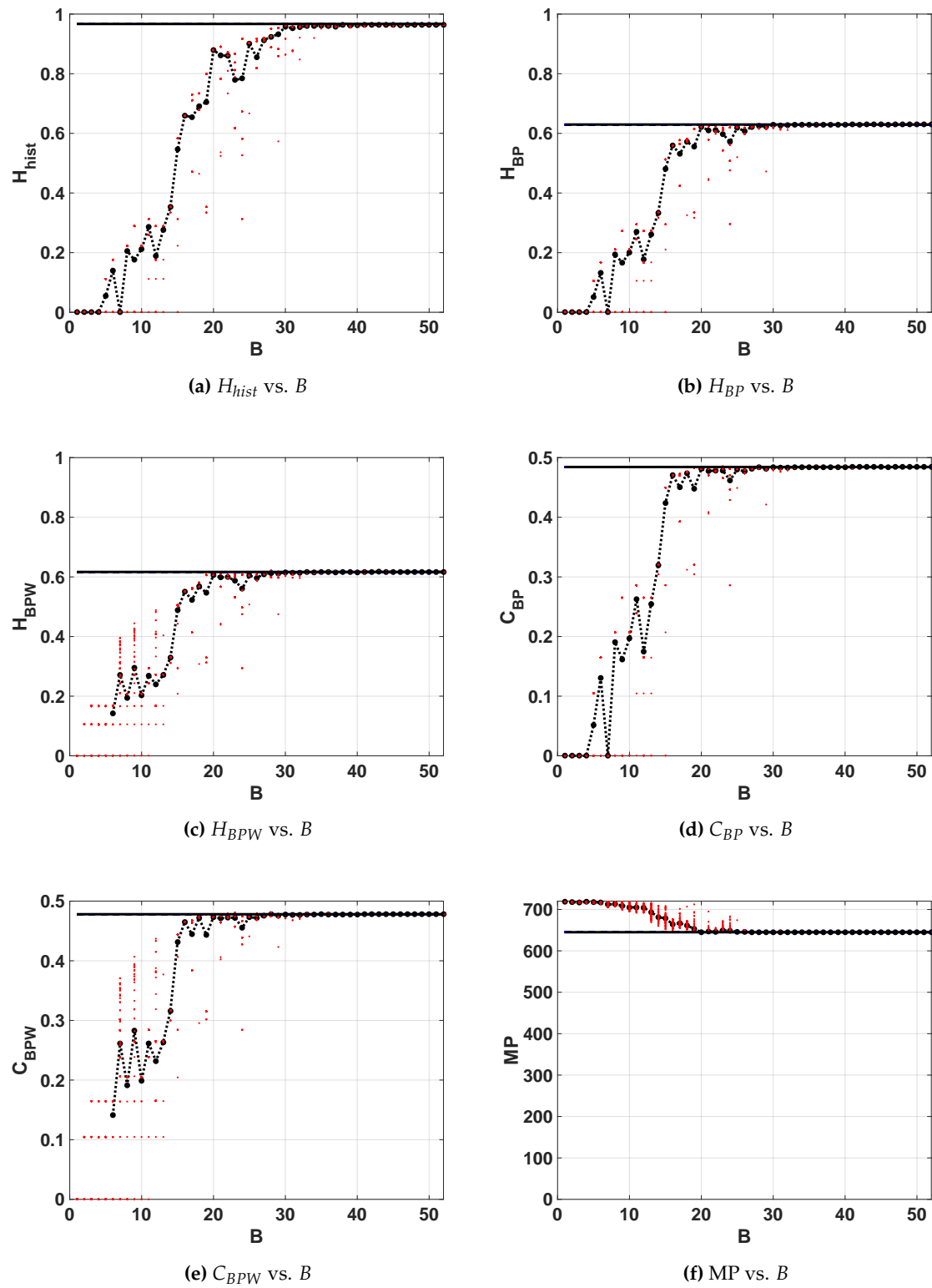


Figure 5. Statistical properties for LOG map as function of B .

The same results are shown in double entropy planes with the precision as parameter (Figure 6a without amplitude contributions and Figure 6b with amplitude contributions). These figures show: 100 red points for each fixed-point precision (B) and their average in black (dashed black line connecting

³³⁸ black dots), 100 blue dots that are the results of each run in floating-point and the black star is their
³³⁹ average. Here, the 100 blue points and their average are overlapped.

³⁴⁰ As expected, the fixed-point architecture implementation converges to the floating-point value
³⁴¹ as B increases. For both planes, $H_{hist} \times H_{BP}$ and $H_{hist} \times H_{BPW}$, from $B = 20$, H_{hist} increases but
³⁴² H_{BP} and H_{BPW} remain constant. It can be seen that the distribution of values reaches high values
³⁴³ ($\langle H_{hist} \rangle = 0.9669$) but their mixing is poor ($\langle H_{BP} \rangle = 0.6269$).

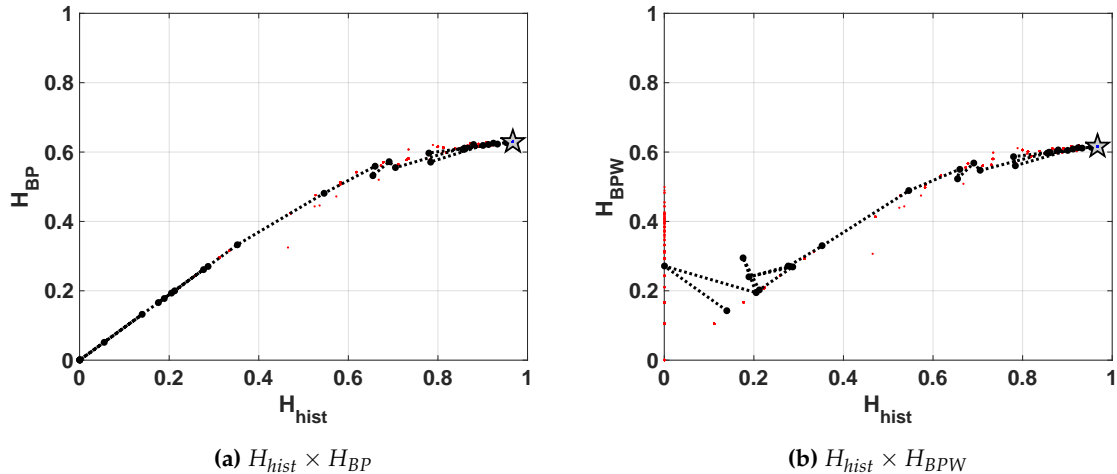


Figure 6. Evolution of statistical properties in double entropy plane for LOG map.

³⁴⁴ In Figure 7a and 7b we show the entropy-complexity planes. Dotted grey lines are the upper
³⁴⁵ and lower margins, it is expected that a chaotic system remains near the upper margin. These results
³⁴⁶ characterize a chaotic behavior, in $H_{BP} \times C_{BP}$ plane we can see a low entropy and high complexity.

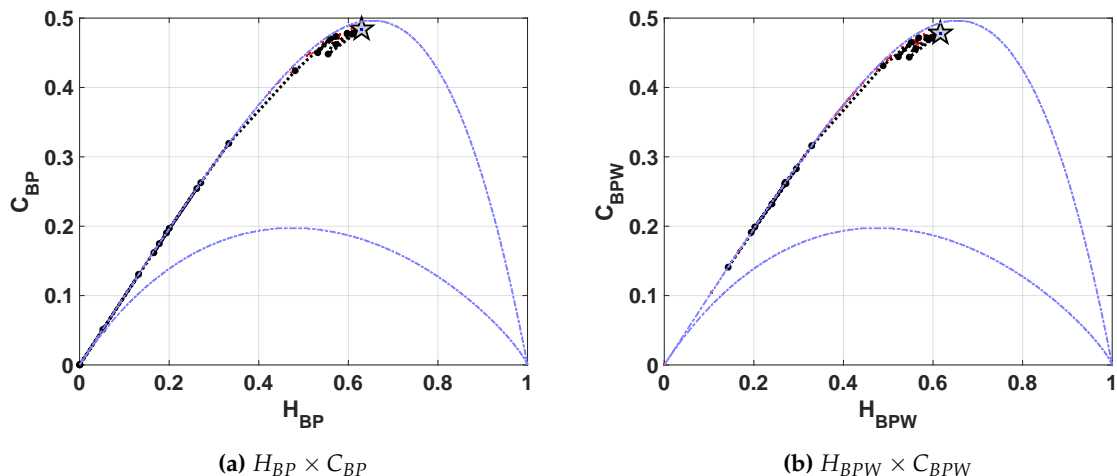


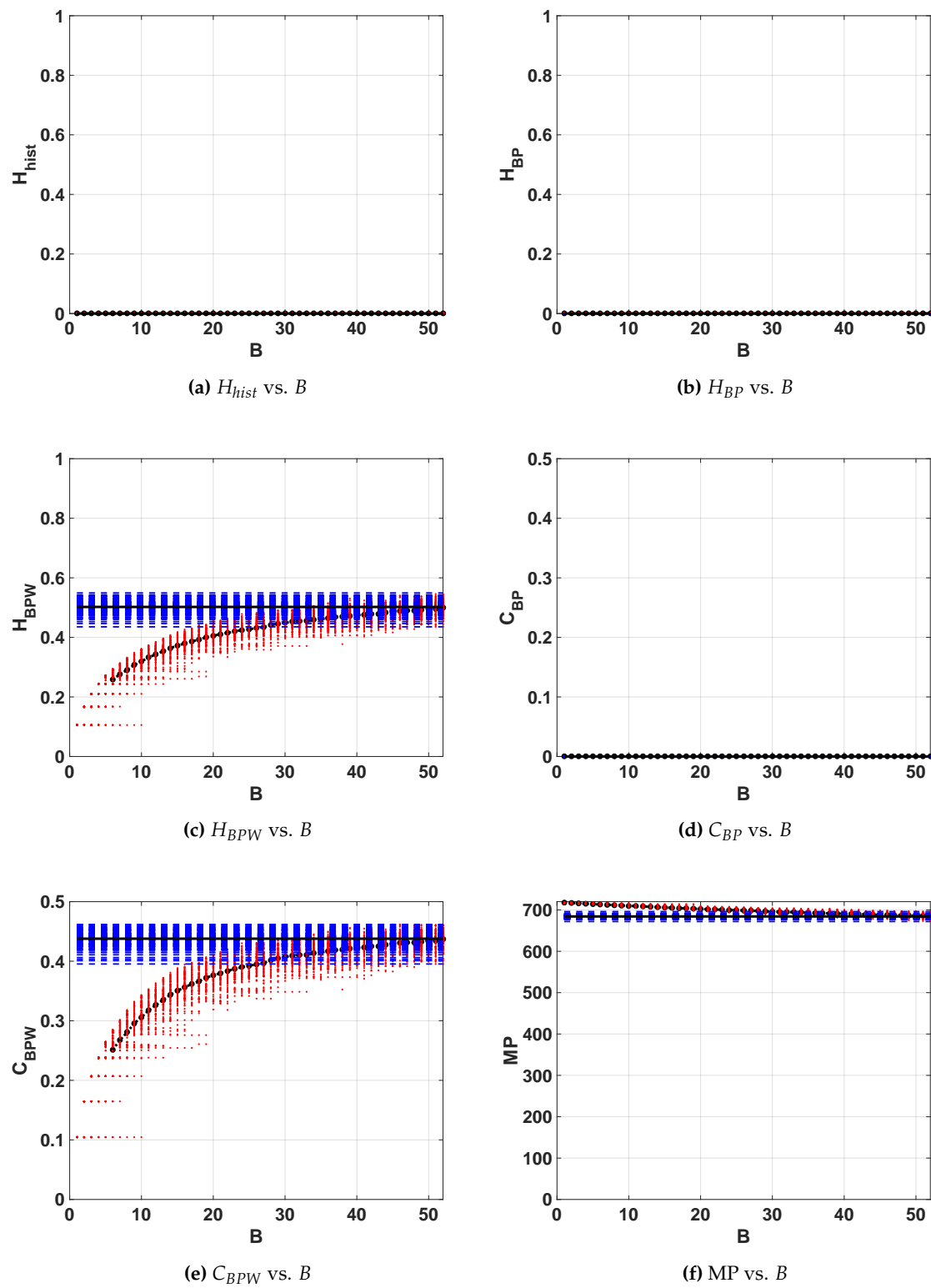
Figure 7. Evolution of statistical properties in causal entropy-complexity plane for LOG map.

³⁴⁷ 3.2.2. TENT

³⁴⁸ When this map is implemented in a computer using any numerical representation system (even
³⁴⁹ floating-point!) truncation errors rapidly increase and make unstable fixed point in $x^* = 0$ to become
³⁵⁰ stable. The sequences within the attractor domain of this fixed point will have a short transitory of
³⁵¹ length between 0 and B followed by an infinite number of 0's [51,52]. This issue is easily explained in

[53], the problem appears because all iterations have a left-shift operation that carries the 0's from the right side of the number to the most significant positions.

Figures 8a to 8f show the quantifiers for floating- and fixed-point numerical representations. H_{hist} , H_{BP} and C_{BP} quantifiers are equal to zero for all precisions, this reflects that the series quickly converge toward a fixed point for every initial conditions. In the case of H_{BPW} and C_{BPW} quantifiers are different to zero because BPW procedure discards the elements once the fixed point is reached. The high dispersions in H_{BPW} , C_{BPW} and MP are related to the short length of serie's transient. These transients that converge to a fixed point have a maximum length of B elements (iterations) for fixed-point arithmetic and 53 for floating-point (IEEE754 double precision).

**Figure 8.** Statistical properties of TENT map.

361 Summarizing, in spite of using a high number of bits (with any 2-based numerical representation)
 362 to represent the digitalized TENT map it always quickly converges to the fixed point in $(x_n, x_{n+1}) =$
 363 $(0, 0)$.

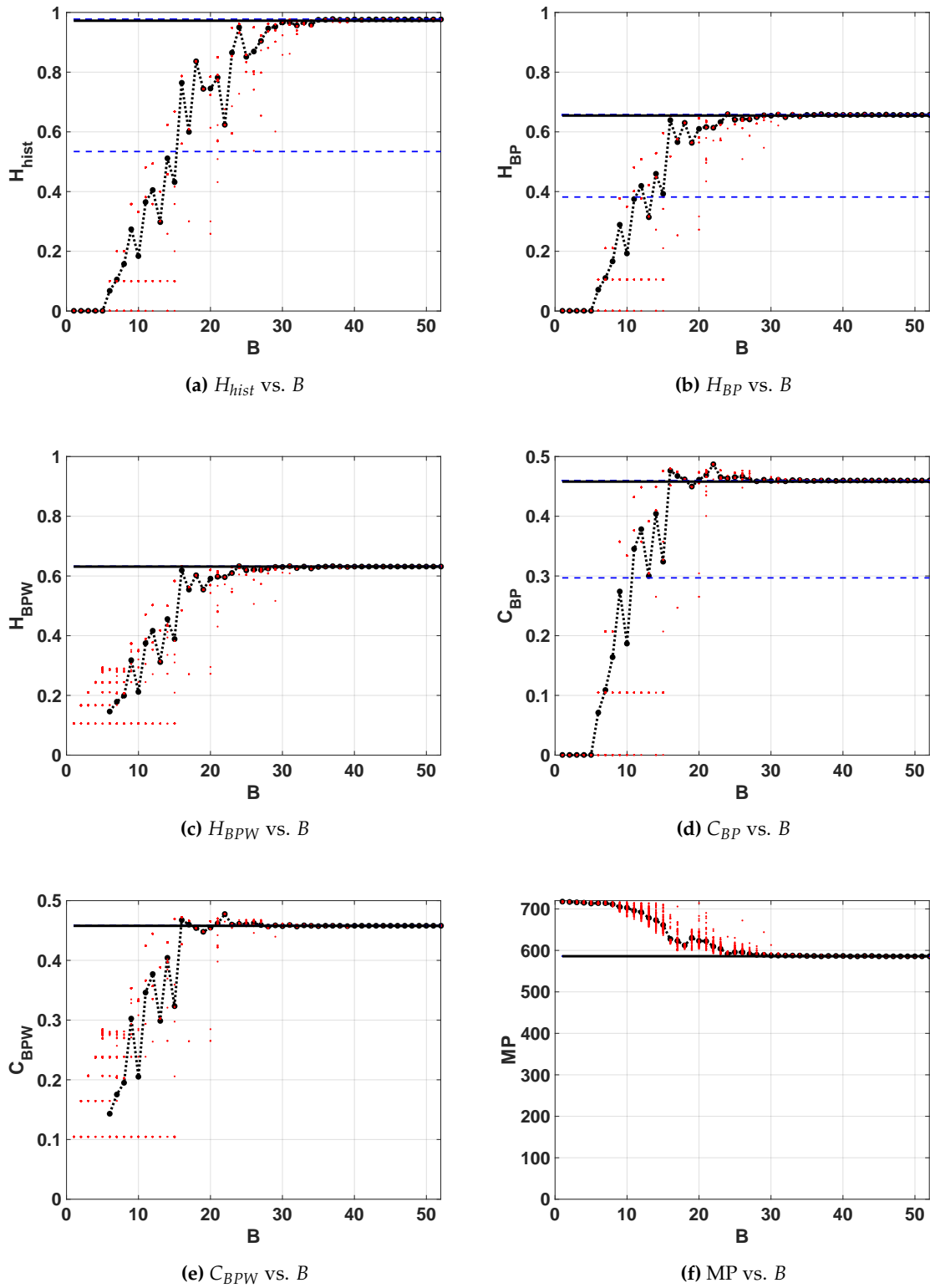
³⁶⁴ 3.3. *Quantifiers of combined Maps*

³⁶⁵ Here we report our results for the three combinations of the combined maps, SWITCH, EVEN
³⁶⁶ and ODD.

³⁶⁷ 3.3.1. SWITCH

³⁶⁸ Results with sequential switching are shown in Figures 9a to 9f. The calculated entropy value for
³⁶⁹ floating-point implementation is $\langle H_{hist} \rangle = 0.9722$, this value is slightly higher than the one obtained for
³⁷⁰ the LOG map. For fixed-point arithmetic this value is reached in $B = 24$, but it stabilizes from $B = 28$.
³⁷¹ Regarding the ordering patterns the number of MP decreases to 586, this value is lower than the one
³⁷² obtained for LOG map. It means the entropy H_{BP} may increase up to $\ln(134) / \ln(720) \simeq 0.74$. BP and
³⁷³ BPW quantifiers reach their maximum of $\langle H_{BP} \rangle = 0.6546$ and $\langle H_{BPW} \rangle = 0.6313$ at $B = 16$, but they
³⁷⁴ stabilize from $B = 24$. Complexities are lower than for LOG, $\langle C_{BP} \rangle = 0.4580$ and $\langle C_{BPW} \rangle = 0.4578$,
³⁷⁵ these values are reached for $B \geq 15$ but they stabilize for $B \geq 23$. Compared with LOG, statistical
³⁷⁶ properties are better with less amount of bits, for $B \geq 24$ this map reaches optimal characteristics in
³⁷⁷ the sense of random source.

³⁷⁸ Furthermore, we encountered one initial condition in floating-point with an anomalous behavior.
³⁷⁹ Figures 9a, 9b and 9d show an horizontal blue dashed line that is far from the average value, unlike this
³⁸⁰ is not detected by quantifiers based on BPW procedure in Figures 9c and 9e. Nevertheless comparing
³⁸¹ both procedures (BP and BPW) we were able to detect a falling to fixed point after a long transitory,
³⁸² the BPW procedure discards the constant values (corresponding with a fixed point) and works only
³⁸³ over the transitory values.

**Figure 9.** Statistical properties of SWITCH map.

³⁸⁴ Double entropy plane $H_{hist} \times H_{BP}$ is showed in Figures 10. The reached point in this plane for
³⁸⁵ SWITCH map is similar to that reached for LOG map, and it is denoted by a star in the figure. The
³⁸⁶ mixing is slight better in this case.

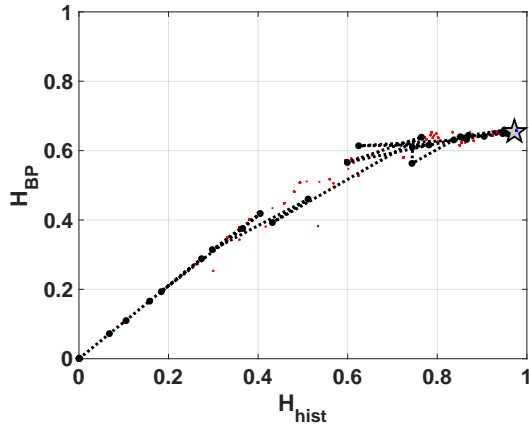


Figure 10. Evolution of statistical properties in double entropy plane for SWITCH map $H_{hist} \times H_{BP}$.

387 Entropy-complexity plane $H_{BP} \times C_{BP}$ is showed in Figures 11. If we compare with the same plane
 388 in the case of LOG (Figures 7a), C_{BP} is lower for SWITCH, this fact shows a more random behavior.

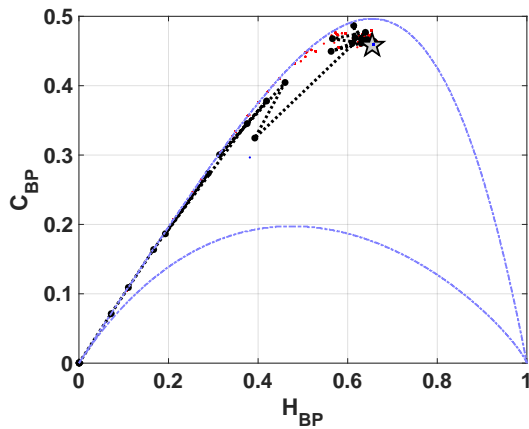


Figure 11. Evolution of statistical properties in causal entropy-complexity plane for SWITCH map $H_{BP} \times C_{BP}$.

389 3.3.2. EVEN and ODD

390 In Figures 12a and 13a we can see that quantifiers related to the normalized histogram of values
 391 slightly degrades with the skipping procedure. For example $\langle H_{hist} \rangle$ reduces from 0.9722 without
 392 skipping to 0.9459 for EVEN and 0.9706 for ODD. This difference between EVEN and ODD in floating
 393 point is because a high dispersion was obtained for H_{hist} , H_{BP} and C_{BP} but not for H_{BPW} or C_{BPW} .

394 Figures 12b to 12f and Figures 13b to 13f show the results of BP and BPW quantifiers for EVEN
 395 and ODD respectively. Higher accuracy is required to achieve lower complexity than without using
 396 skipping. From the MP point of view a great improvement is obtained using any of the skipping
 397 strategies but ODD is slightly better than EVEN. Missing patterns are reduced to $MP = 118$ for EVEN
 398 and ODD, increasing the maximum allowed Bandt & Pompe entropy that reaches the mean value
 399 $\langle H_{BP} \rangle = 0.8381$ for EVEN, and $\langle H_{BP} \rangle = 0.9094$. The complexity is reduced to $\langle C_{BP} \rangle = 0.224$ for EVEN
 400 and $\langle C_{BP} \rangle = 0.282$ for ODD. The minimum number of bits to converge to this value is $B > 40$ for both
 401 EVEN and ODD maps.

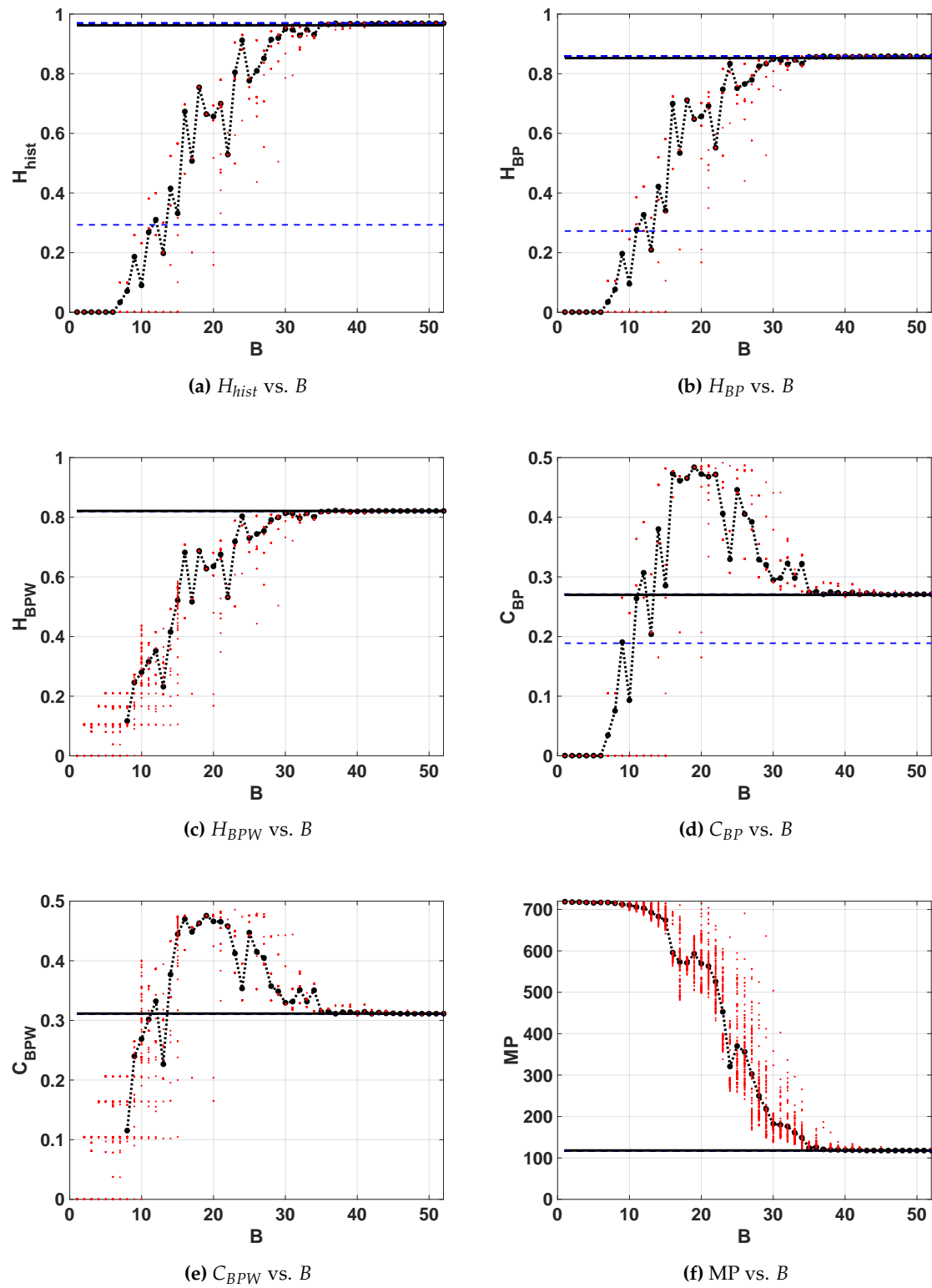
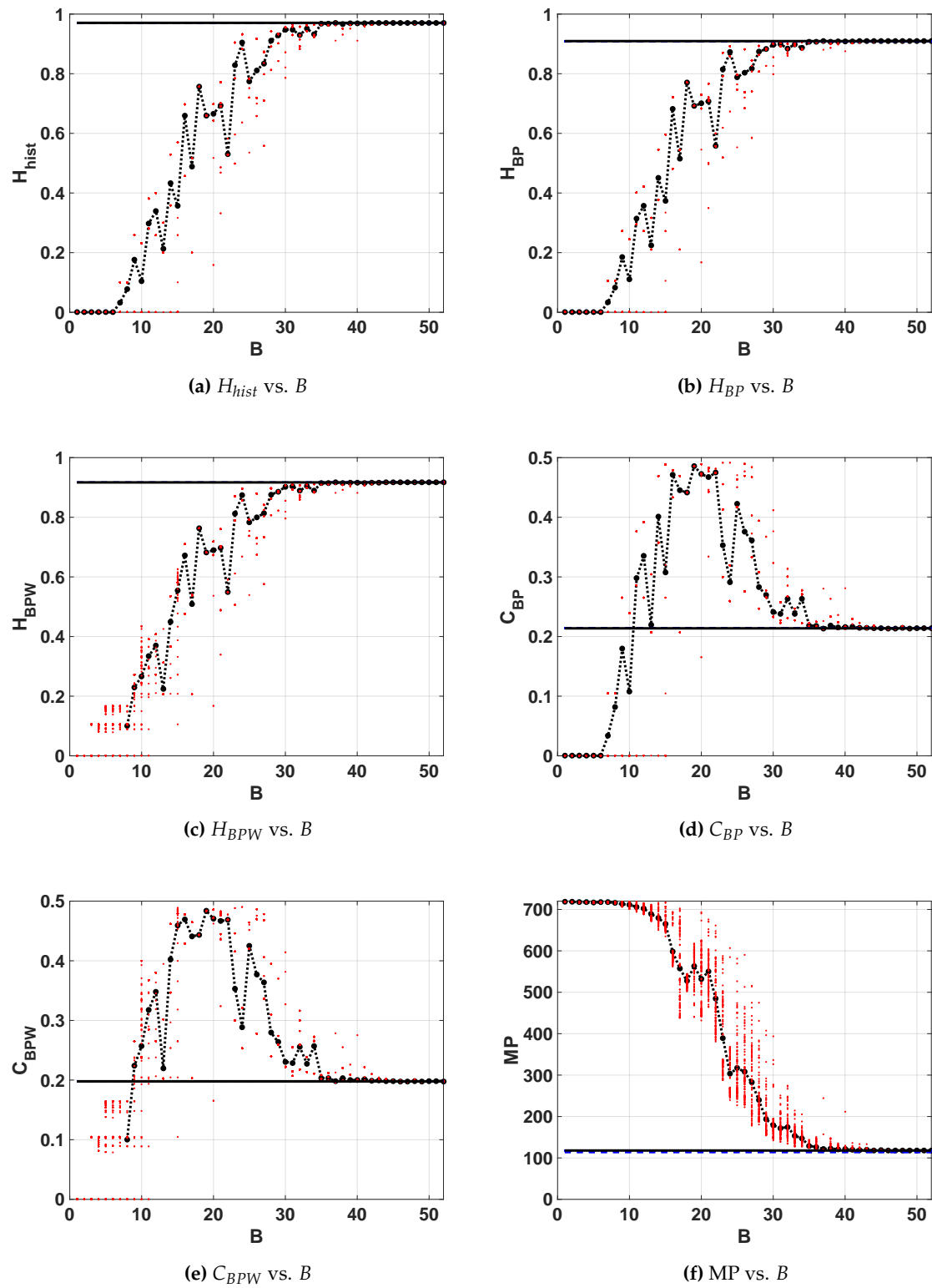


Figure 12. Statistical properties of EVEN map.

**Figure 13.** Statistical properties of ODD map.

The enhancement showed in Figures 12 and 13 is reflected in the position of asymptotic point in the planes 14, and 15. In both cases this position is closest to the ideal point $(H_{hist}, H_{BP}) = (1, 1)$, because the resulting vectors present better mixing.

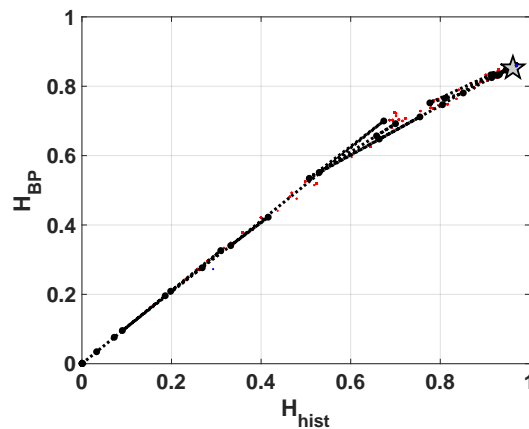


Figure 14. Evolution of statistical properties in double entropy plane for EVEN map $H_{hist} \times H_{BP}$.

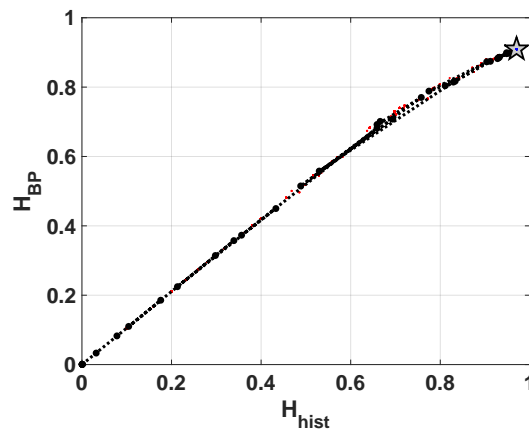


Figure 15. Evolution of statistical properties in double entropy plane for ODD map $H_{hist} \times H_{BP}$.

Compatible results are shown in Figures 16 and 17, the position of asymptotic point is closest to the ideal point $(H_{hist}, H_{BP}) = (1, 0)$. This result reflects that mixing is better because the complexity of resulting system is lower. This plane detects that the vector generated by ODD skipping is more mixed than EVEN.

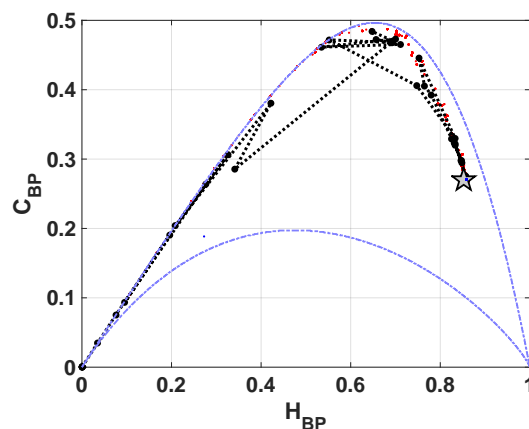


Figure 16. Evolution of statistical properties in entropy-complexity plane for EVEN map $H_{BP} \times C_{BP}$.

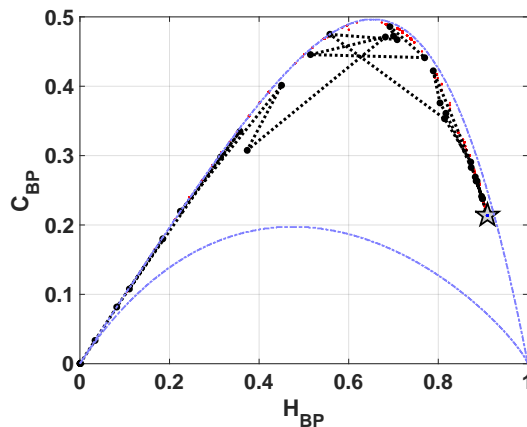


Figure 17. Evolution of statistical properties in entropy-complexity plane for ODD map $H_{BP} \times C_{BP}$.

409 4. Conclusions

410 In this paper we explored the statistical degradation of simple, switched and skipped chaotic
 411 maps due to the inherent error of a based-2 systems. We evaluated mixing and amplitude distributions
 412 from a statistical point of view.

413 Our work complements previous results given in [14], where period lengths were investigated. In
 414 that sense, our results were compatible with these. We can see that the switching between two maps
 415 increases the dependence of period as function of precision, this is because the correlation length is
 416 also increased. Nevertheless, the standard procedure of skipping reduce the period length in almost a
 417 half.

418 All statistics of the maps represented in fixed-point produces a non-monotonous evolution toward
 419 the floating-point results. This result is relevant because it shows that increasing the precision is not
 420 always recommended.

421 It is specially interesting to note that some systems (TENT) with very nice statistical properties in
 422 the real numbers world, become "pathological" when binary numerical representations are used. As a
 423 rule, if a map is generated only by shift operations (it depends on the base of the arithmetic logic unit
 424 and the map itself), all initial conditions will converge to a fixed point with a transient no longer than
 425 the length of the mantissa being used.

426 By comparing between BP and BPW quantifiers, we were able to detect falls to fixed points and to
 427 estimate the relative length of transient. It can be seen in all implementations of TENT, in one initial
 428 condition of SWITCH and EVEN for floating-point implementation.

429 Related to statistical behavior, our results show that SWITCH has a marginal improvement in
 430 the mixing with respect to LOG (and TENT, of course). However the greatest improvement comes
 431 when skipping is applied, we can see that BP and BPW entropies grow and BP and BPW complexities
 432 decrease, for the same numerical representation. This result is relevant because evidences that a long
 433 period is not synonymous of good statistics, switched maps EVEN and ODD have half period lengths
 434 but their mixing is better and their amplitude distributions remain almost equal. As counterpart, more
 435 precision is needed to reach the better asymptotes that offers the switching method.

436 **Acknowledgments:** This work was partially supported by the Consejo Nacional de Investigaciones Científicas y
 437 Técnicas (CONICET), Faculty of Engineering of the National University of Mar del Plata (FI-UNMDP) and the
 438 International Centre for Theoretical Physics (ICTP) Associateship Scheme.

439 References

- 440 1. Machado, R.F.; Baptista, M.S.; Grebogi, C. Cryptography with chaos at the physical level. *Chaos, Solitons*
 441 and *Fractals* **2004**, *21*, 1265–1269.

- 442 2. Smaoui, N.; Kanso, A. Cryptography with chaos and shadowing. *Chaos, Solitons and Fractals* **2009**,
443 *42*, 2312–2321.
- 444 3. De Micco, L.; Antonelli, M.; Larrondo, H. Stochastic degradation of the fixed-point version of 2D-chaotic
445 maps. *Chaos, Solitons and Fractals* **2017**, *104*, 477–484.
- 446 4. Antonelli, M.; Micco, L.D.; Gonzalez, C.M.; Larrondo, H.A. Analysis of the digital implementation of a
447 chaotic deterministic-stochastic attractor. 2012 Argentine School of Micro-Nanoelectronics, Technology
448 and Applications (EAMTA), 2012, pp. 73–78.
- 449 5. De Micco, L.; Petrocelli, R.A.; Larrondo, H.A. Constant Envelope Wideband Signals using Arbitrary
450 Chaotic Maps. *Proceedings of XII RPIC 2007*.
- 451 6. De Micco, L.; Arizmendi, C.M.; Larrondo, H.A. Zipping characterization of chaotic sequences used in
452 spread spectrum communication systems. *Institute of Physics Conference Proceedings 913* **2007**, pp. 139–144.
- 453 7. Alcover, P.M. Moiré interferences in the map of orbits of the Mandelbrot Set. *Commun. Nonlinear Sci.
454 Numer. Simul.* **2017**, *42*, 545–559.
- 455 8. Dias, S.P.; Longa, L.; Curado, E. Influence of the finite precision on the simulations of discrete dynamical
456 systems. *Commun. Nonlinear Sci. Numer. Simul.* **2011**, *16*, 1574–1579.
- 457 9. Azzaz, M.S.; Tanougast, C.; Sadoudi, S.; Bouridane, A. Synchronized hybrid chaotic generators: Application
458 to real-time wireless speech encryption. *Commun. Nonlinear Sci. Numer. Simul.* **2013**, *18*, 2035–2047.
- 459 10. Nepomuceno, E.G.; Mendes, E.M. On the analysis of pseudo-orbits of continuous chaotic nonlinear systems
460 simulated using discretization schemes in a digital computer. *Chaos, Solitons and Fractals* **2017**, *95*, 21–32.
- 461 11. Liao, S. On the numerical simulation of propagation of micro-level inherent uncertainty for chaotic
462 dynamic systems. *Chaos, Solitons and Fractals* **2013**, *47*, 1–12.
- 463 12. Grebogi, C.; Ott, E.; Yorke, J.A. Roundoff-induced periodicity and the correlation dimension of chaotic
464 attractors. *Phys. Rev. A* **1988**, *38*, 3688–3692.
- 465 13. Persohn, K.J.; Povinelli, R.J. Analyzing logistic map pseudorandom number generators for periodicity
466 induced by finite precision floating-point representation. *Chaos, Solitons and Fractals* **2012**, *45*, 238–245.
- 467 14. Nagaraj, N.; Shastry, M.C.; Vaidya, P.G. Increasing average period lengths by switching of robust chaos
468 maps in finite precision. *Eur. Phys. J. Spec. Top.* **2008**, *165*, 73–83.
- 469 15. Liu, X.; Teo, K.L.; Zhang, H.; Chen, G. Switching control of linear systems for generating chaos. *Fractals An
470 Interdiscip. J. Complex Geom. Nat.* **2006**, *30*, 725–733.
- 471 16. Gluskin, E. The nonlinear-by-switching systems (a heuristic discussion of some basic singular systems)
472 **2008**. [[0801.3652](#)].
- 473 17. Zarlenga, D.G.; Larrondo, H.A.; Arizmendi, C.M.; Family, F. Complex synchronization structure of an
474 overdamped ratchet with discontinuous periodic forcing. *Phys. Rev. E - Stat. Nonlinear, Soft Matter Phys.*
475 **2009**, *80*, 011127.
- 476 18. Chiou, J.S.; Cheng, C.M. Stabilization analysis of the switched discrete-time systems using Lyapunov
477 stability theorem and genetic algorithm. *Chaos, Solitons and Fractals* **2009**, *42*, 751–759.
- 478 19. Borah, M.; Roy, B.K. An enhanced multi-wing fractional-order chaotic system with coexisting attractors
479 and switching hybrid synchronisation with its nonautonomous counterpart. *Chaos, Solitons and Fractals*
480 **2017**, *102*, 372–386.
- 481 20. De Micco, L.; Larrondo, H.A.; Plastino, A.; Rosso, O.A. Quantifiers for randomness of chaotic
482 pseudo-random number generators. *Philos. Trans. A. Math. Phys. Eng. Sci.* **2009**, *367*, 3281–3296,
483 [[0812.2250](#)].
- 484 21. Bandt, C.; Pompe, B. Permutation entropy: a natural complexity measure for time series. *Phys. Rev. Lett.*
485 **2002**, *88*, 174102.
- 486 22. Rosso, O.A.; Larrondo, H.A.; Martin, M.T.; Plastino, A.; Fuentes, M.A. Distinguishing Noise from Chaos.
487 *Phys. Rev. Lett.* **2007**, *99*, 154102.
- 488 23. De Micco, L.; González, C.M.; Larrondo, H.A.; Martin, M.T.; Plastino, A.; Rosso, O.A. Randomizing
489 nonlinear maps via symbolic dynamics. *Phys. A Stat. Mech. its Appl.* **2008**, *387*, 3373–3383.
- 490 24. De Micco, L.; Fernández, J.G.; Larrondo, H.A.; Plastino, A.; Rosso, O.A. Sampling period, statistical
491 complexity, and chaotic attractors. *Phys. A Stat. Mech. its Appl.* **2012**, *391*, 2564–2575.
- 492 25. Rosso, O.A.; Larrondo, H.A.; Martín, M.T.; Plastino, A.; Fuentes, M.A. Distinguishing noise from chaos.
493 *Physical Review Letters* **2007**, *99*, 154102, [[1401.2139](#)].

- 494 26. Rosso, O.A.; De Micco, L.; Larrondo, H.A.; Martin, M.T.; Plastino, A. Generalized Statistical Complexity
495 Measure. *Int. J. Bifurc. Chaos* **2010**, *20*, 775.
- 496 27. Antonelli, M.; De Micco, L.; Larrondo, H.A. Measuring the jitter of ring oscillators by means of information
497 theory quantifiers. *Commun. Nonlinear Sci. Numer. Simul.* **2017**, *43*, 139–150.
- 498 28. Fadlallah, B.; Chen, B.; Keil, A.; Príncipe, J. Weighted-permutation entropy: A complexity measure for time
499 series incorporating amplitude information. *Phys. Rev. E - Stat. Nonlinear, Soft Matter Phys.* **2013**, *87*, 1–7.
- 500 29. Amigó, J.M.; Zambrano, S.; Sanjuán, M.A.F. True and false forbidden patterns in deterministic and random
501 dynamics. *Europhys. Lett.* **2007**, *79*, 50001.
- 502 30. Rosso, O.A.; Carpi, L.C.; Saco, P.M.; Ravetti, M.G.; Larrondo, H.A.; Plastino, A. The Amigo paradigm of
503 forbidden/missing patterns: A detailed analysis. *Eur. Phys. J. B* **2012**, *85*.
- 504 31. Shannon, C.E.; Weaver, W. The mathematical theory of communication. *Bell Syst. Tech. J.* **1948**, *27*, 379–423.
- 505 32. Kantz, H.; Kurths, J.; G., M.K. *Nonlinear Analysis of Physiological Data / Springer Science & Business Media*;
506 Springer, 2012; p. 344.
- 507 33. Feldman, D.P.; McTague, C.S.; Crutchfield, J.P. The organization of intrinsic computation:
508 Complexity-entropy diagrams and the diversity of natural information processing. *Chaos* **2008**, *18*, 043106,
509 [[0806.4789](#)].
- 510 34. Lamberti, P.W.; Martin, M.T.; Plastino, A.; Rosso, O.A. Intensive entropic non-triviality measure. *Phys. A
511 Stat. Mech. its Appl.* **2004**, *334*, 119–131.
- 512 35. López-Ruiz, R.; Mancini, H.L.; Calbet, X.; L6pez-Ruiz, R.; Mancini, H.L.; Calbet ', X. A statistical measure
513 of complexity. *Phys. Lett. A* **1995**, *209*, 321–326.
- 514 36. Martin, M.T.; Plastino, A.; Rosso, O.A. Statistical complexity and disequilibrium. *Phys. Lett. Sect. A Gen.
515 At. Solid State Phys.* **2003**, *311*, 126–132.
- 516 37. Grosse, I.; Bernaola-Galvn, P.; Carpena, P.; Rom??n-Rold??n, R.; Oliver, J.; Stanley, H.E. Analysis of
517 symbolic sequences using the Jensen-Shannon divergence. *Phys. Rev. E. Stat. Nonlin. Soft Matter Phys.* **2002**, *65*, 16.
- 518 38. Martin, M.T.; Plastino, A.; Rosso, O.A. Generalized statistical complexity measures: Geometrical and
519 analytical properties. *Phys. A Stat. Mech. its Appl.* **2006**, *369*, 439–462.
- 520 39. Rosso, O.A.; Zunino, L.; P??rez, D.G.; Figliola, A.; Larrondo, H.A.; Garavaglia, M.; Mart??n, M.T.; Plastino,
521 A. Extracting features of Gaussian self-similar stochastic processes via the Bandt-Pompe approach. *Phys.
522 Rev. E - Stat. Nonlinear, Soft Matter Phys.* **2007**, *76*, 061114.
- 523 40. Anteneodo, C.; Plastino, A.R. Some features of the L??pez-Ruiz-Mancini-Calbet (LMC) statistical measure
524 of complexity. *Phys. Lett. Sect. A Gen. At. Solid State Phys.* **1996**, *223*, 348–354.
- 525 41. Olivares, F.; Plastino, A.; Rosso, O.A. Contrasting chaos with noise via local versus global information
526 quantifiers, 2012.
- 527 42. González, C.M.; Larrondo, H.A.; Rosso, O.A. Statistical complexity measure of pseudorandom bit
528 generators. *Phys. A Stat. Mech. its Appl.* **2005**, *354*, 281–300.
- 529 43. Amigó, J.M.; Kocarev, L.; Szczepanski, J. Order patterns and chaos. *Phys. Lett. Sect. A Gen. At. Solid State
530 Phys.* **2006**, *355*, 27–31.
- 531 44. Amigó, J.M.; Kocarev, L.; Tomovski, I. Discrete entropy. *Phys. D Nonlinear Phenom.* **2007**, *228*, 77–85.
- 532 45. Amigó, J.M.; Zambrano, S.; Sanjuán, M.A.F. Combinatorial detection of determinism in noisy time series.
533 *Europhys. Lett.* **2008**, *83*, 60005.
- 534 46. Amigó, J. *Permutation Complexity in Dynamical Systems*; Springer Series in Synergetics, Springer Berlin
535 Heidelberg: Berlin, Heidelberg, 2010; pp. 195–197, [[arXiv:1011.1669v3](#)].
- 536 47. Micco, L.D.; Antonelli, M.; Larrondo, H.A.; Boemo, E. Ro-based PRNG: FPGA implementation and
537 stochastic analysis **2014**. pp. 1–6.
- 538 48. Wackerbauer, R.; Witt, A.; Atmanspacher, H.; Kurths, J.; Scheingraber, H. A comparative classification of
539 complexity measures. *Chaos, Solitons and Fractals* **1994**, *4*, 133–173.
- 540 49. Antonelli, M.; Micco, L.D.; Larrondo, H. Causal and non-causal entropy quantifiers implemented in FPGA
541 **2016**. pp. 1–5.
- 542 50. Lasota, A.; Mackey, M.C. *Chaos, fractals, and noise : stochastic aspects of dynamics*; Number 97, Springer-Verlag,
543 1994; pp. xiv, 472 p.
- 544 51. Jessa, M. The period of sequences generated by tent-like maps. *IEEE Trans. Circuits Syst. I Fundam. Theory
545 Appl.* **2002**, *49*, 84–89.

- 547 52. Callegari, S.; Setti, G.; Langlois, P. A CMOS tailed tent map for the generation of uniformly distributed
548 chaotic sequences. Proc. 1997 IEEE Int. Symp. Circuits Syst. Circuits Syst. Inf. Age ISCAS '97. IEEE, 2013,
549 Vol. 2, pp. 781–784, [[1302.0511](#)].
550 53. Li, S. When Chaos Meets Computers, 2004, [[arXiv:nlin/0405038](#)].

551 © 2017 by the authors. Submitted to *Entropy* for possible open access publication under the terms and conditions
552 of the Creative Commons Attribution (CC BY) license (<http://creativecommons.org/licenses/by/4.0/>).